

11-1-2008

Electronic structure and transmission characteristics of SiGe nanowires

Neerav Kharche

Purdue University - Main Campus

Mathieu Luisier

Purdue University - Main Campus

Timothy B. Boykin

University of Alabama, Huntsville

Gerhard Klimeck

Purdue University - Main Campus, gekco@purdue.edu

Follow this and additional works at: <http://docs.lib.purdue.edu/nanodocs>

Kharche, Neerav; Luisier, Mathieu; Boykin, Timothy B.; and Klimeck, Gerhard, "Electronic structure and transmission characteristics of SiGe nanowires" (2008). *Other Nanotechnology Publications*. Paper 76.

<http://docs.lib.purdue.edu/nanodocs/76>

This document has been made available through Purdue e-Pubs, a service of the Purdue University Libraries. Please contact epubs@purdue.edu for additional information.

Electronic structure and transmission characteristics of SiGe nanowires

Neerav Kharche · Mathieu Luisier ·
Timothy B. Boykin · Gerhard Klimeck

© Springer Science+Business Media LLC 2008

Abstract Atomistic disorder such as alloy disorder, surface roughness and inhomogeneous strain are known to influence electronic structure and charge transport. Scaling of device dimensions to the nanometer regime enhances the effects of disorder on device characteristics and the need for atomistic modeling arises. In this work SiGe alloy nanowires are studied from two different points of view: (1) Electronic structure where the bandstructure of a nanowire is obtained by projecting out small cell bands from a supercell eigen-spectrum and (2) Transport where the transmission coefficient through the nanowire is computed using an atomistic wave function approach. The nearest neighbor $sp^3d^5s^*$ semi-empirical tight-binding model is employed for both electronic structure and transport. The connection between dispersions and transmission coefficients of SiGe random alloy nanowires of different sizes is highlighted. Localization is observed in thin disordered wires and a transition to bulk-like behavior is observed with increasing wire diameter.

Keywords Nanowires · SiGe · Brillouin zone-unfolding · Open boundary conditions · NEGF

1 Introduction

Semiconductor nanowires are believed to be the potential candidates for devices at the end of the roadmap. Recently several groups have demonstrated the nanowire field-effect transistors (FETs) fabricated from pure elemental or compound semiconductors like Si [1], Ge [2], and GaAs [3] as well as semiconductor alloys like SiGe [4], and their III–V counterparts. Random semiconductor alloy nanowires have local atomic and inhomogeneous strain disorder. Traditional methods like virtual crystal approximation (VCA) give poor results even for the bulk alloys like AlGaAs [5]. The effects of disorder will be more pronounced at the nanoscale and more rigorous models are required to study the effect of random disorder. Moreover, as the nanowire dimension shrinks to below around 5 nm, the effective mass approximation breaks down [6] and an atomistic representation of the material is needed for transport calculations.

This work presents the electronic structure and transport calculations for SiGe nanowires that contain strain, position, and atom disorder. Square nanowire cross-sections ranging from 2 to 7 nm are simulated to study the effect of disorder. Strain and electronic structure calculations are performed on the whole nanowire in free standing configuration and substrate is not taken into account.

2 Method

The translational symmetry is broken in semiconductor alloy nanowires due to random placement of atoms and inho-

N. Kharche (✉) · G. Klimeck
Network for Computational Nanotechnology, Purdue University,
West Lafayette, IN 47906, USA
e-mail: nkharce@purdue.edu

G. Klimeck
Jet Propulsion Laboratory, California Institute of Technology,
Pasadena, CA 91109, USA

M. Luisier
Integrated Systems Laboratory, ETH Zürich, 8092 Zürich,
Switzerland

T.B. Boykin
Department of Electrical and Computer Engineering, University
of Alabama, Huntsville, AL 35899, USA

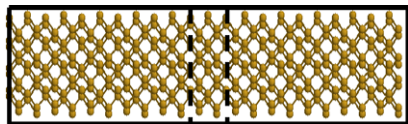


Fig. 1 Two equivalent representations of a [100] Si nanowire. Small cell representation in which a wire is made up of a smallest repeating unit i.e. 4 atomic planes thick slab. Supercell representation in which a repeating unit consists of integer number of small cells. Here, nanowire supercell (*solid lines*) consists of 11 small cells (*dotted lines*)

mogeneous strain. Thus one runs into the problem of choosing a unit cell for the bandstructure calculation. One way to take alloy disorder into account is to work with longer supercells (Fig. 1) as basic repeating units. The nanowire bandstructure obtained from the supercell calculation is folded. Atomistic disorder along the wire breaks the translational symmetry and the concept of bandstructure can only be considered in an approximate sense. In this work, the one dimensional version of the zone-unfolding method [7] is used to project out the approximate eigenspectrum of the nanowire supercell on the small cell Brillouin-Zone. The Projected probabilities are then used to extract the bandstructure of the alloy nanowire according the probability sum rule for band counting [5]. The small cell bandstructure thus obtained captures the effect of SiGe alloy disorder on the electronic structure.

Alternatively to the bandstructure view we also model coherent transport through the wire. A scattering boundary method [8] is used to calculate the open boundary conditions at both ends of the nanowire. The transmission coefficients through the nanowire are then computed by using a hybrid method combining a recursive Non-Equilibrium Greens Function (NEGF) and a wavefunction method [8]. The scattering boundary method calculates the surface Green's function from the bandstructure of a reservoir. In these calculations the semi-infinite source (drain) region is assumed to be identical to the first (last) slab of the nanowire. That is the same atomic disorder as the first (last) slab is assumed to repeat throughout the semi-infinite source (drain) region so that the bandstructure of the source (drain) region is same as that of the first (last) slab. The tight-binding model in which atom and strain disorders are automatically incorporated by the atomistic nature of the Hamiltonian is used.

3 Results

The free standing square cross section $\text{Si}_{0.8}\text{Ge}_{0.2}$ alloy nanowires studied here have two types of disorders: random atom disorder due to alloying and inhomogeneous strain disorder due to different Si-Si, Ge-Ge, and Si-Ge bond lengths. The nanowire geometry is specified in terms of conventional Zincblende (cubic) unit cells as $n_x \times n_y \times n_z$ where n_α is

the number of cubes in direction- α . All electronic structure and transport calculations have been done in $\text{sp}^3\text{d}^5\text{s}^*$ tight-binding model. Relaxed wire geometries are calculated in NEMO-3D [10–12] from Valance Force Field approach [9]. The bulk and strain Si and Ge parameters are taken from [13, 14].

The smaller wire (Fig. 2) has the dimensions of $40 \times 6 \times 6$ ($22.3 \times 3.3 \times 3.3$ nm) i.e. it is constructed from $40 \times 6 \times 6$ slabs along [100] crystallographic direction. Electronic structure of this nanowire is calculated with NEMO-3D in 3 different formulations in Fig. 2(a). The first approach is the so called local bandstructure approach in which the bandstructure of each slab is calculated assuming that this slab repeats infinitely along the nanowire. Due to fluctuations in atomic arrangements along the nanowire length one expects to see the different bandstructures for each slab as shown in Fig. 2(a). This local bandstructure approach does not deliver a meaningful overall bandedge of the wire or a meaningful effective mass. The second approach is the conventional VCA approach which averages the atom potentials according to the atomic composition of the material. This results in a homogeneous wire without any disorder. The bandstructure might then as well be represented by a single slab. In the third approach eigenspectrum of the whole nanowire supercell is unfolded to obtain the bandstructure of the best translationally symmetric nanowire small cell.

Figure 2(b) shows the transmission coefficient through this wire computed using coupled open boundary conditions and atomistic NEGF approach. Transmission coefficient shows the noisy behavior because of random SiGe alloy disorder and inhomogeneous strain disorder in the wire. Steps in the transmission plot can be roughly related to the unfolded bandstructure (Fig. 2(a)) from supercell calculations. Four separate Δ_4 valley bands appear as a single band with a finite energy spread in the projected bandstructure. These four bands turn on near 1.44 eV which corresponds to the conduction band transmission turn on. Two Δ_2 valley bands turn on near 1.47 eV which leads to a step in the transmission. Four more channels due to higher Δ_4 valley sub-bands turn on near 1.57 eV. These transmission features can not be related to the conventional virtual crystal approximation (VCA) bandstructure shown in Fig. 2(a).

Peaks in the transmission plot can be related to resonant transport through localized states in the wire. Local band-edge plots of the lowest Δ_4 and Δ_2 valley minima are shown in Fig. 2(c). Variation of band-edges along the nanowire length cause reflections which lead to the formation of the localized states and peaks in transmission as seen in the density of states and transmission plots. Note that the presence of the peaks in the transmission can not be predicted from the unfolded bandstructure because the unfolded bandstructure is an eigenspectrum of the best possible translationally symmetric Hamiltonian through the nanowire.

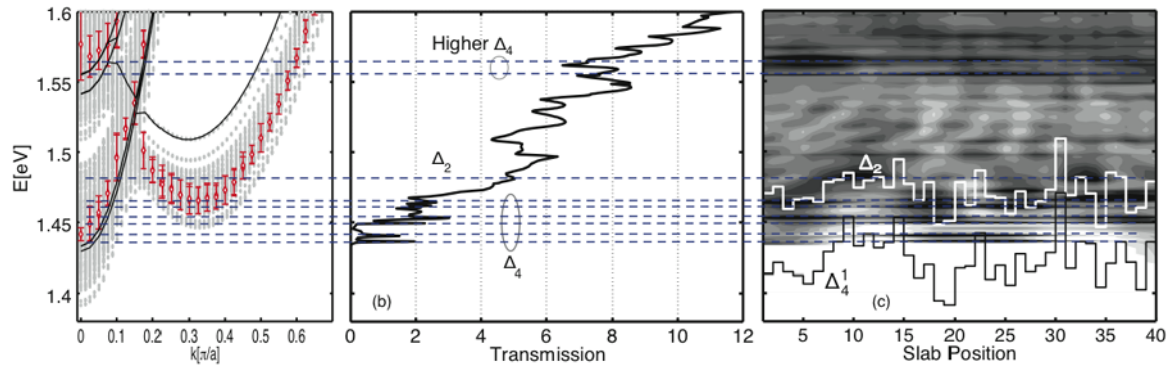
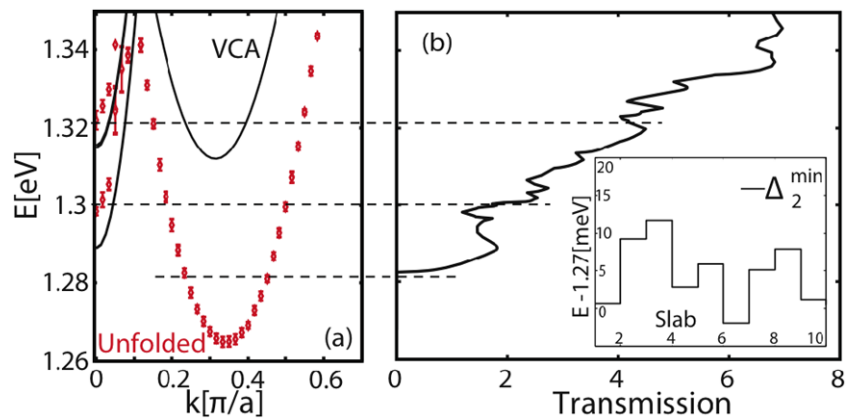


Fig. 2 (Color online) (a) Bandstructures of $40 \times 6 \times 6$ $\text{Si}_{0.8}\text{Ge}_{0.2}$ alloy nanowire in local bandstructure (gray), VCA (black) and zone-unfolding (red) formulations. (b) Transmission coefficient. Steps in transmission are identified as resulting from new bands appearing in projected bandstructure. (c) Local band-edge of lowest energy Δ_4

and Δ_2 valley minima along wire length and density of states (on a log scale). Peaks in the transmission arising from Δ_4 valley localized states have dominant DOS contributions coming from $|p_y|^2 + |p_z|^2$ while Δ_2 valley peaks have dominant $|p_x|^2$ contribution

Fig. 3 (Color online) (a) Bandstructures of $60 \times 13 \times 13$ $\text{Si}_{0.8}\text{Ge}_{0.2}$ alloy nanowire in VCA (black) and zone-unfolding (blue) formulations. (b) Transmission characteristics of the wire. Inset shows the local Δ_2 valley minima near the left reservoir



As the nanowire cross section increases random distribution of Ge atoms is expected to have less influence on the transport characteristic of the SiGe nanowires. The local bandstructure variations along the length of the nanowire reduce which reduce the number of localized states. The bandstructure and the transmission characteristics of a $60 \times 13 \times 13$ ($32.5 \times 7.1 \times 7.1$ nm) $\text{Si}_{0.8}\text{Ge}_{0.2}$ wire are shown in Fig. 3. Error bars on the approximate bandstructure are smaller compared to smaller cross section nanowire of Fig. 2. The transmission coefficient also shows smoother step like behavior compared to the smaller nanowire. The transmission behavior of the nanowire can not be predicted from the VCA bandstructure because the transmission turns on at 1.28 eV before the first VCA band which only starts at 1.29 eV. The minimum energy valleys in the VCA formalism are Δ_4 valleys. The local conduction band-minimum along the wire, however, is Δ_2 like (inset of Fig. 3(b)) which agrees with the unfolded bandstructure. Thus as opposed to the VCA, the unfolded bandstructure correctly predicts relative positions of valley minima.

It is important to point out here that the bandstructure calculation and the transport calculation use different bound-

ary conditions. In the bandstructure calculation the wire is repeated infinitely with disorder, while the transport calculation assumes a homogeneous ordered alloy at the band-edges as injectors. The transmission turn on occurs at higher energies than predicted by the unfolded bandstructure because the local conduction band minima near the left reservoir (also the source of injected waves) are higher in energy which prevent propagation waves with energies lower than 1.28 eV.

Extracted band parameters such as conduction band minima, effective masses and average band uncertainties are plotted as a function of the nanowire size in Fig. 4. The approximate bandstructure predicts a smaller Δ_2 bandminimum than the VCA similar to AlGaAs nanowires [15] and AlGaAs bulk [5]. The direct (Δ_4) and indirect (Δ_2) valley-bandgaps show an interesting cross-over for wires with sizes larger than 4 nm, which will significantly increase the density of states at the conduction band edge and influence device performance; the VCA assumption does not result in such a cross-over. The VCA and unfolded bandstructure effective masses are slightly different (Fig. 4(b)). Unfolded bandstructure effective masses of larger cross section

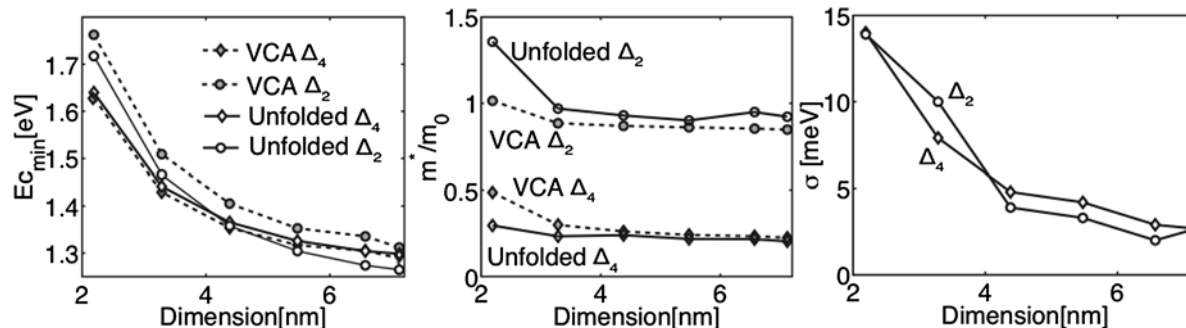


Fig. 4 (a) Direct (Δ_4 valleys) and indirect (Δ_2 valleys) conduction band minima obtained from VCA and zone-unfolded bandstructures. (b) Effective masses of Δ_4 and Δ_2 valleys. (c) Energy uncertainties of Δ_4 and Δ_2 bands

nanowires are closer to the bulk $\text{Si}_{0.8}\text{Ge}_{0.2}$ Γ - and X -valley effective masses ($0.92m_0$ and $0.19m_0$ respectively) reported in [16] compared to VCA. More accurate effective masses and bandedges obtained from the zone-unfolding method can be used in simple ballistic MOSFET transport models such as the top-of-the barrier model of [17].

Since the unfolded supercell bandstructure is approximate it has an error bar associated with each energy and wavevector in the dispersion. These energy uncertainties can be used to calculate the scattering time of the state according to the prescription of [18]. As the nanowire cross-section increases the error bars become smaller (Fig. 4(c)) and the system becomes more bulk like.

4 Conclusion

The electronic structure and the transport characteristics of random SiGe alloy nanowires indicate the critical importance of the treatment of atomistic disorder. Typical approaches of a smoothed out material (VCA) or considerations of bandstructure in just individual slices clearly fail to represent the disordered nanowire physics especially for very narrow cross section nanowires. Unfolded bandstructures from zone-unfolding of the supercell eigenspectrum and transmission characteristics combined, are shown to explain the relevant physics in these disordered systems. As the nanowire cross-section increases the transport behavior moves from resonance dominated regime to a smoother ideal 1D transport regime.

Acknowledgements This work was supported by Semiconductor Research Corporation. Calculations were performed on nanoHUB.org resources provided by the Network for Computational Nanotechnology, funded by the National Science Foundation.

References

- Cui, Y., Lauhon, L.J., Gudiksen, M.S., Wang, J., Lieber, C.M.: Diameter-controlled synthesis of single-crystal silicon nanowires. *Appl. Phys. Lett.* **78**, 2214 (2001)
- Greytak, A.B., Lauhon, L.J., Gudiksen, M.S., Lieber, C.M.: Growth and transport properties of complementary germanium nanowire field-effect transistors. *Appl. Phys. Lett.* **84**, 4176 (2004)
- Persson, A.I., Larsson, M.W., Steinström, S., Ohlsson, B.J., Samuelson, L., Wallenberg, L.R.: Solid-phase diffusion mechanism for GaAs nanowire growth. *Nat. Mater.* **3**, 677 (2004)
- Kim, C.-J., Yang, J.-E., Lee, H.-S., Jang, H.M., Joa, M.-H., Park, W.-H., Kim, Z.H., Maeng, S.: Fabrication of $\text{Si}_{1-x}\text{Ge}_x$ alloy nanowire field-effect transistors. *Appl. Phys. Lett.* **91**, 033104 (2007)
- Boykin, T.B., Klimeck, G.: Practical application of zone-folding concepts in tight-binding. *Phys. Rev. B* **71**, 115215 (2005)
- Boykin, T.B., Kharche, N., Klimeck, G., Korkusinski, M.: Approximate bandstructures of semiconductor alloys from tight-binding supercell calculations. *J. Phys. Condens. Mater.* **19**, 036203 (2007)
- Wang, J., Rahman, A., Ghosh, A., Klimeck, G., Lundstrom, M.: On the validity of the parabolic effective-mass approximation for the current-voltage calculation of silicon nanowire transistors. *IEEE Trans. Electron Devices* **52**(7), 1589 (2005)
- Luisier, M., Schenk, A., Fichtner, W., Klimeck, G.: Atomistic simulation of nanowires in the $sp^3d^5s^*$ tight-binding formalism: from boundary conditions to strain calculations. *Phys. Rev. B* **74**, 205323 (2006)
- Keating, P.N.: Effect of invariance requirements on the elastic strain energy of crystals with application to the diamond structure. *Phys. Rev.* **145**, 637 (1966)
- Klimeck, G., Oyafuso, F., Boykin, T.B., Bowen, R.C., von Allmen, P.: Development of a nanoelectronic 3-D (NEMO 3-D) simulator for multimillion atom simulations and its application to alloyed quantum dots. *Comput. Model. Eng. Sci.* **3**(5), 601 (2002)
- Klimeck, G., Ahmed, S., Bae, H., Kharche, N., Clark, S., Haley, B., Lee, S., Naumov, M., Ryu, H., Saied, F., Prada, M., Korkusinski, M., Boykin, T.B.: Atomistic simulation of realistically sized nanodevices using NEMO 3-D: part I—Models and benchmarks. *IEEE Trans. Electron Devices* **54**(9), 2079 (2007)
- Klimeck, G., Ahmed, S., Kharche, N., Korkusinski, M., Usman, M., Prada, M., Boykin, T.B.: Atomistic simulation of realistically sized nanodevices using NEMO 3-D: part II—Applications. *IEEE Trans. Electron Devices* **54**(9), 2090 (2007)
- Boykin, T.B., Klimeck, G., Oyafuso, F.: Valence band effective mass expressions in the $sp^3d^5s^*$ empirical tight-binding model applied to a new Si and Ge parameterization. *Phys. Rev. B* **69**, 115201 (2004)
- Boykin, T.B., Kharche, N., Klimeck, G.: Brillouin zone unfolding of perfect supercells composed of non-equivalent primitive cells. *Phys. Rev. B* **76**, 035310 (2007)

15. Boykin, T.B., Luisier, M., Schenk, A., Kharche, N., Klimeck, G.: The electronic structure and transmission characteristics of disordered AlGaAs nanowires. *IEEE Trans. Nanotechnol.* **6**(1), 43 (2007)
16. Schaffler, F.: In: Levinshstein, M.E., Rumyantsev, S.L., Shur, M.S. (eds.) *Properties of Advanced Semiconductor Materials GaN, AlN, InN, BN, SiC, SiGe*, pp. 149–188. Wiley, New York (2001)
17. Rahman, A., Guo, J., Datta, S., Lundstrom, M.: Theory of ballistic nanotransistors. *IEEE Trans. Electron Devices* **50**, 1853 (2003)
18. Boykin, T.B., Kharche, N., Klimeck, G.: Evolution time and energy uncertainty. *Eur. J. Phys.* **28**, 673 (2007)